

# Thermo-Mechanical Process-Induced Residual Stresses and Deformation Analysis During Manufacturing of Hull Structure

*Tensiones residuales termo mecánicas inducidas por el proceso y análisis de deformación durante la fabricación de la estructura del casco*

*Tensões residuais induzidas pelo processo termo-mecânico e análise de deformação durante a fabricação da estrutura do casco*

Saad Ahmed<sup>1</sup>, Muhammad Asif<sup>2,\*</sup>, Asad Ali Zaidi<sup>3</sup>

Recibido: 13/05/2024

Aceptado: 09/10/2024

**Summary.** - Hull structures such as stiffened plates and thin panels are the building blocks of ship structures, and therefore understanding their manufacturing process is of utmost importance. The welding process has been widely used to join stiffeners, stringers, and girders onto the plate. The thermo-mechanical loading and constraints during the welding process generally induced deformations and residual stresses. A deep understanding of the process parameters during thermo-mechanical processing is required to control the process-induced deformation. Therefore, this study aims to investigate the deformation and thermal stress generation in hull structures (panels/stiffened plates) during thermo-mechanical processes such as welding. A finite element modeling approach was proposed while incorporating the thermal and nonlinear thermo-elastic-plastic material behavior. The thin panels with different geometrical configurations and boundary conditions were simulated using steady state and transient heat-transfer-stress deformations analysis to simulate real-life scenarios. Both modeling approaches give a useful insight into understanding the complex nature of deformation and built-up residual stresses. However, the transient heat transfer-stress deformation analysis results were found in a reasonably good agreement with experimental data.

**Keywords:** Hull structure, welding deformations, finite element analysis, residual stresses, transient heat transfer.

---

(\*) Corresponding Author

<sup>1</sup> MSc Student, Department of Naval Architecture, Pakistan Navy Engineering College, National University of Sciences and Technology Pakistan, sahed.mech@gmail.com, ORCID iD: <https://orcid.org/0009-0005-4851-788X>

<sup>2</sup> Associate Professor, Department of Engineering Sciences, Pakistan Navy Engineering College, National University of Sciences and Technology Pakistan, muhammadasif@pnec.nust.edu.pk, ORCID iD: <https://orcid.org/0000-0003-4318-8253>

<sup>3</sup> Associate Professor, Department of Mechanical Engineering, Faculty of Engineering, Islamic University of Madinah, P.O. Box 170, Madinah, Saudi Arabia, sali@iu.edu.sa, ORCID iD: <https://orcid.org/0000-0001-5457-5684>

**Resumen.** - Las estructuras de casco, como las placas rígidas y los paneles delgados, son los componentes básicos de las estructuras de barco y, por lo tanto, comprender su proceso de fabricación es de suma importancia. El proceso de soldadura se ha utilizado ampliamente para unirse a los rígidos, largueros y vigas en la placa. La carga y restricciones termo mecánicas durante el proceso de soldadura generalmente indujeron deformaciones y tensiones residuales. Se requiere una comprensión profunda de los parámetros del proceso durante el procesamiento termo-mecánico para controlar la deformación inducida por el proceso. Por lo tanto, este estudio tiene como objetivo investigar la generación de deformación y estrés térmico en estructuras de casco (paneles/placas rígidas) durante los procesos termo-mecánicos como la soldadura. Se propuso un enfoque de modelado de elementos finitos al incorporar el comportamiento de material térmico y no lineal de plástico termoelástico. Los paneles delgados con diferentes configuraciones geométricas y condiciones de contorno se simularon utilizando un análisis de deformaciones de estrés por calor de calor transitorio y transitorio para simular escenarios de la vida real. Ambos enfoques de modelado brindan una visión útil de comprender la naturaleza compleja de la deformación y las tensiones residuales acumuladas. Sin embargo, los resultados del análisis de deformación de transferencia de calor transitorio de calor se encontraron en un acuerdo razonablemente bueno con los datos experimentales.

**Palabras clave:** Estructura del casco, deformaciones de soldadura, análisis de elementos finitos, tensiones residuales, transferencia de calor transitorio.

**Resumo.** - Estruturas de casco, como placas rígidas e painéis finos, são os blocos de construção das estruturas de navios e, portanto, entender seu processo de fabricação é de extrema importância. O processo de soldagem tem sido amplamente utilizado para unir reforços, longarinas e vigas no prato. A carga termo-mecânica e as restrições durante o processo de soldagem geralmente induziam deformações e tensões residuais. É necessário um profundo entendimento dos parâmetros do processo durante o processamento termo-mecânico para controlar a deformação induzida pelo processo. Portanto, este estudo tem como objetivo investigar a deformação e a geração de tensão térmica em estruturas de casco (painéis/placas rígidas) durante processos termo-mecânicos, como soldagem. Uma abordagem de modelagem de elementos finitos foi proposta ao incorporar o comportamento do material termoelástico-elástico térmico e não linear. Os painéis finos com diferentes configurações geométricas e condições de contorno foram simuladas usando análise de deformações de estresse de transferência de transferência transitória para simular cenários da vida real. Ambas as abordagens de modelagem fornecem uma visão útil sobre a compreensão da natureza complexa da deformação e das tensões residuais construídas. No entanto, os resultados da análise de deformação transitória por transferência de calor de transferência de calor foram encontrados em uma concordância razoavelmente boa com dados experimentais.

**Palavras-chave:** Estrutura do casco, deformações de soldagem, análise de elementos finitos, tensões residuais, transferência transitória de calor.

**1. Introduction .** - The Stiffened panel is the building block in the marine, aerospace, and offshore industry [1]. The most common joining process used to manufacture stiffened panels is welding. Unfortunately, welding comes with unavoidable deformation and residual stresses due to shrinkage of material near the area adjacent to welding seams during the process. The ship industry faces many challenges in controlling the distortion and deformation in hull during the fabrication process. Therefore, a deep understanding of the manufacturing process and parameters that govern the deformation is of utmost importance. Exploring the causes of deformation due to thermal stresses on stiffened panels will help to design processes that yield panels with controlled state of the deformation. The evaluation of strength analysis, longitudinal bending moments, and controlling deformation plays a vital role in a vessel's quality and longevity.

Welding is an integral part of the assembly and fabrication process. The welding process usually induced the unwanted deformations in structure and effects the component's structural integrity [2, 3]. Therefore, accurate evaluation of the deformation in stiffened panels is an essential part of ship structure manufacturing. To counter the adverse effects of welding induced deformation, the welding engineer consider many factors such as the sequence of weld [4], welding parameters, and mechanical constraints to reduce deformation and production cost. In addition, the welding induced deformations are affected by design factors such as types of joints, panel thickness, stiffener arrangement, temperature-dependent material properties, and manufacturing factors that include the welding method, speed, intensity, clamping and joint strategy [5, 7].

Several authors employed finite element analysis (FEA) with thermo-elasto-plastic models to investigate the welding induced distortions with different design and manufacturing factors. Kumar et al. [8] investigated distortion in a thin plate due to the bead-on joint. Chen et al. studied the buckling and distortion defects in fillet welds [9]. They considered section-integration shell elements and the effects of the welding sequence on the stiffened panels was investigated. Zhang et al. [10] studied the influence of welding mechanical boundary condition on the residual stress and distortion of a stiffened panel. These fixtures were to affect the location of deformation and magnitude of thermal stresses. To simplify the stiffened plates' design and analysis, the two-dimensional constant stress distribution along the length were considered. However, this reduces the accuracy of the results but understanding the factors affecting the out-of-plane displacement, shrinkage, and angular displacement, an FEA numerical model was developed to investigate the behavior. This approach was found to help predict the deformation in an earlier phase, which would save time and cost of production.

The FEA is the most popular analysis method but not the only way to model the welding process. In literature [11], several other methods such as the inherent strain method (ISM) and equivalent load method (ELM) was also proposed. The ISM was found to be capable of predicting the size of the heat-affected zone and applied inherent strain values by substituting equivalent elastic force to evaluate deformation. The ISM has some advantage but FEA was considered an easier and more powerful approach but sometime computationally expensive [12]. The processing time of numerical simulations was reduced by an efficient method proposed using composite shell elements based on inherent strain method [13]. Similarly, the approaches like Swarm Optimization (PSO) and grid search (GS) showed good potential to predict welding deformation and thermal stresses [14] but computationally very challenging for large scale problems.

A ship panel experiences tensile, compression, and axial loads, and moreover the thermo-mechanical material behavior play an important role in designing the stiffened panels. Steel is a primary material for shipbuilding in the world for its low cost and high flexibility in fabrication. In a detailed review, Zhang et al [15] ultimate strength of steel plates and stiffened panels under axial compression. Wang et al. [16] showed that the strength of the material depends on temperature. At higher temperature, the Q460 steel shows lower strength loss than mild steel Ali et al. [17] showed that the ship panels made of grade A36 and A131 have the best suitable properties for stiffened panels. There is extensive research ongoing to develop stronger, lighter, and economical materials for ship structures. Semi-steel and composite material have enhanced resistance collision capabilities and can be potentially beneficial [18]. There is a correlation between material properties and welding joints. Higher yield strength materials generate larger transverse shrinkage angular deformation, and longitudinal deflection[19]. Russell [20] reveals that almost 25% of total labor cost in fabrication is usually served in the rectification of deformation in ship hull structure during the fabrication

process. This is a serious problem and affects the overall cost of the ship due to extra rectification work. They also discussed how laser welding can prove more beneficial than regular arc welding. McPherson [21] showed that 80% of the total distortion can be reduced by efficient management in the fabrication process, while 20% is due to the presence of residual stress, which requires more complex solutions.

Another study addresses the challenge of thermal deformation in aluminum hulls during welding. By simulating various welding sequences using finite element methods, it demonstrates that optimizing these conditions can reduce maximum displacement by up to 52.1% and effective plastic strain by up to 19.6%, thereby enhancing structural integrity and sustainability in the marine industry [31].

Welding induced deformations are an inevitable part of the manufacturing process and is a big concern for the shipbuilding industry. Researchers are continuously devising new numerical methods and modeling techniques that can help significantly to understand the cause and thus remedy of welding induced deformations.

Similarly, [32] introduces a distortion simulator that employs finite element methods (FEM) to predict welding and buckling distortion in shipbuilding. The tool allows for quick predictions without requiring extensive expertise and achieves 80-98% accuracy when validated against commercial software and measured data, underscoring the effectiveness of FEM in predicting welding deformation.

This study proposes a transient thermal-elastic-plastic FEA numerical model to predict the deformation and residual stresses generated during the welding process of yacht panels. Different boundary conditions and design parameters were considered, such as welding speed, natural convection, and cooling time and their influence on welding distortions and thermal residual stress were investigated. In the end, some interesting conclusions and future directions were discussed.

**2. Methodology.** - Figure 1 shows the structural components hierarchy of the hull structure. At the lowest scale, the thin plate is usually reinforced with different stiffeners to form a stiffened plate. Then, the combinations of different stiffened plates will yield a panel and several panels will lead to the deck of the hull structure. In this study we mainly developed a numerical model for the stiffened yacht panel. The numerical model of the panel structure includes a thin plate, a girder, and a multiple stiffener arrangement are analyzed using three different methodologies.

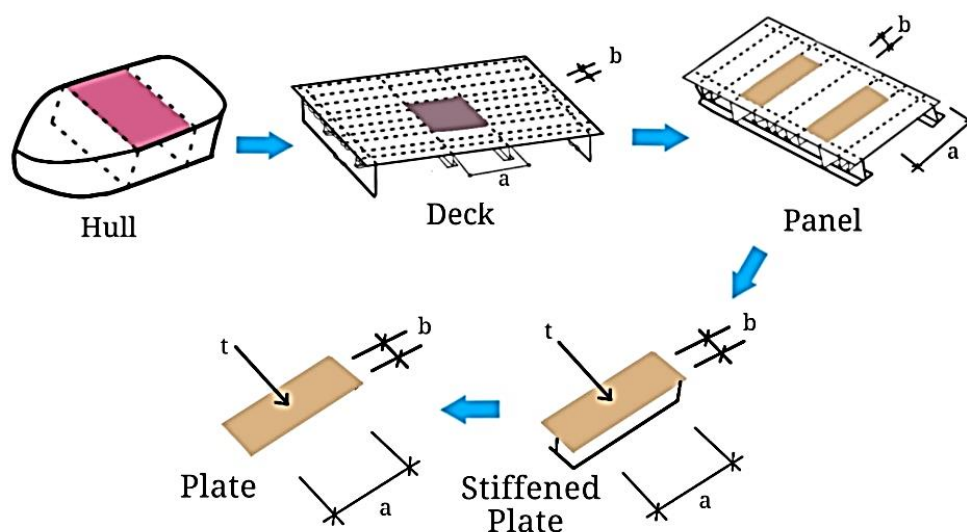


Figure 1. Structural components hierarchy of the hull structure

**2.1. Thermo-Mechanical Modeling Procedure.** - All numerical simulations were performed using ANSYS software. The numerical solution was obtained by performing numerical simulations using three different methodologies. Each with its unique set of boundary conditions and loads to capture the physics behind the process. These are presented in more detail in the next section. In addition to thermo-mechanical loading case, the sequential coupling of the thermal model with the structural model were also used. The typical numerical simulation process adopted in this study is shown in Figure 2. First, the steady state or transient heat transfer thermal analysis was performed, which simulated the idealized and more realistic welding process. The temperature fields acquired were then used as the external load on the mechanical model [11]. Thermal expansion and non-uniform shrinkage will generate internal stresses, strains, and distortions.

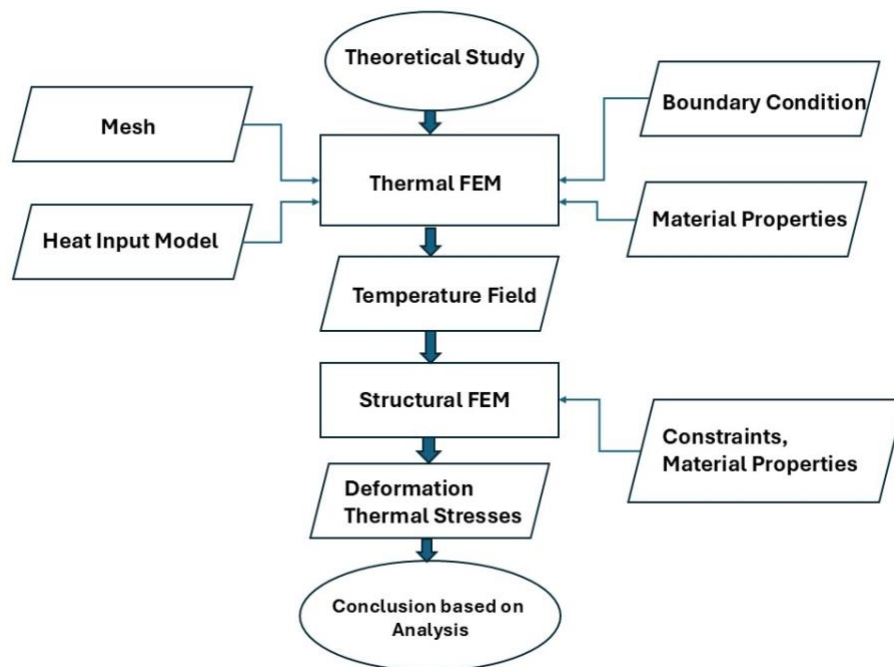


Figure II. Numerical Simulation Process

**2.2. Thermal Analysis.** - The temperature field at each node during the welding process on the welding seam is acquired by solving the non-linear mathematical model depicted in equation 1. The thermal loads achieved are transient in nature.

$$\rho c_p \frac{\partial T}{\partial \tau} = \frac{\partial}{\partial x} \left( k_x \frac{\partial T}{\partial x} \right) + \frac{\partial}{\partial y} \left( k_y \frac{\partial T}{\partial y} \right) + \frac{\partial}{\partial z} \left( k_z \frac{\partial T}{\partial z} \right) + \dot{q} \quad (1)$$

Here,  $C_p$  is the specific heat that signifies the total energy needed to establish the specimen's required temperature gradient [10]. It represents the conservation of energy and is written in a differential form which includes distributed volume, heat flux, and specific heat. The governing equation uses a cartesian coordinate system.  $K_x$ ,  $K_y$ , and  $K_z$  represent thermal conductivities. " $\tau$ " is time, " $\dot{q}$ " is total heat input present in a moving Gaussian heat source. Equation (1) is solved by using equation (2) with boundary conditions [22] and the heat source. To simplify the analysis, we ignored the radiation boundary condition.

$$-\left( k_x \frac{\partial T}{\partial x} n_x + k_y \frac{\partial T}{\partial y} n_y + k_z \frac{\partial T}{\partial z} n_z \right) = q_{\text{conv}} + q_{\text{rad}} - \alpha q_r \quad (2)$$

**2.3. Heat Source.** - The heat source is one of the key input parameters for any welding process. Various mathematical models are used in the literature to represent different types of welding processes. A 3D Gaussian heat source model is typically used to model laser or electron beams. Similarly, Goldak's double ellipsoid heat source model was used for

arc welding. To capture the penetration effect, the front and rear ellipsoid can be calibrated. In this study heat input was given by equation (3) with  $\eta$  denote the welding efficiency, I and U represent current and voltage, respectively [23].

$$Q = \eta UI \quad (3)$$

The double ellipsoid heat model's power intensities that include the front and rear quadrant are given in Equations (4) & (5) [22].

$$q_f(x, y, z) = \frac{6\sqrt{3}f_f Q}{bc a_f \pi \sqrt{\pi}} \cdot e^{-3\frac{x^2}{a_f^2}} \cdot e^{-3\frac{y^2}{b^2}} \cdot e^{-3\frac{z^2}{c^2}} \quad (4)$$

$$q_r(x, y, z) = \frac{6\sqrt{3}f_r Q}{bc a_r \pi \sqrt{\pi}} \cdot e^{-3\frac{x^2}{a_r^2}} \cdot e^{-3\frac{y^2}{b^2}} \cdot e^{-3\frac{z^2}{c^2}} \quad (5)$$

Here, Q is the rate of energy input,  $f_f$  and  $f_r$  are the fractional factors representing the total heat deposited,  $a_f$ ,  $a_r$ ,  $b$  and  $c$  are constant heat source parameters. The values are  $a_f = 5\text{mm}$ ,  $a_r = 20\text{ mm}$ ,  $b = 5\text{ mm}$ ,  $c = 8\text{ mm}$ .

A 3D Gaussian heat energy source uses the following heat model, which is the governing equation used in this study numerical simulations [24].

$$E = C_2 e^{-\frac{[(x-x_0)^2+(y-y_0)^2]}{C_1^2}} \cdot e^{-AC(z-z_0)} \quad (6)$$

Where E = heat energy,  $C_1$  = radius of the beam,  $C_2$  = source power intensity, AC is an absorption coefficient, the  $(x_0, y_0, z_0)$  represents the instantaneous coordinates of the center point of moving heat flux on its designated 'path'. The total distance is simply " $v \times t$ " from the initial point. Here, " $v$ " represents the velocity of the moving heat source, and " $t$ " is time. Beer-Lambert Law governs the energy transferred to the specified material at a certain " $z$ " depth. This heat source model is applied in ANSYS in a time-stepped transient thermal analysis. The coordinates are changed with the corresponding time step. These time steps are calculated via welding speed and length of welding seams.

**2.4. Boundary Conditions.** - Boundary conditions plays a pivotal role in modeling. Ideally, we aimed to apply the conditions as close as real-life scenarios. Three different sets of boundary conditions were used. The first boundary condition was the temperature field at any given point on the surface.  $T_s$  was the temperature on the boundary [10].

$$Ts = Ts(x, y, z, t) \quad (7)$$

The moving heat flux qualified as a second boundary condition at any point on the surface.

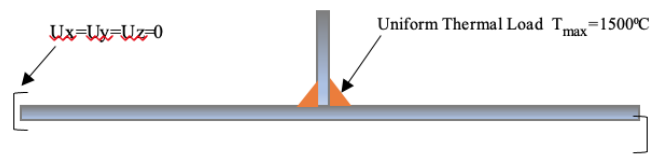
$$-\lambda \frac{\delta T}{\delta n} = qs(x, y, z, t) \quad (8)$$

To increase the authenticity of the simulation, the natural convection by the surrounding media was introduced, which was the third boundary condition. The convection law of heat stated that the "Heat flux density from the surface object to the surrounding in unit time is directly proportional to the temperature difference between them".

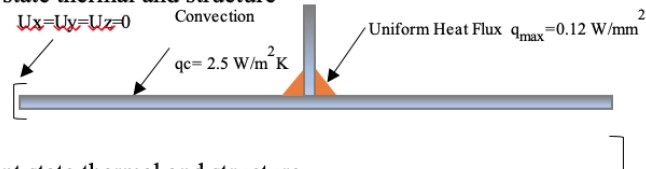
$$-\lambda \frac{\delta T}{\delta n} = \alpha(Ts - Ta) \quad (9)$$

Where  $T_a$  is the ambient temperature,  $\alpha$  is the convection heat transfer coefficient. Three boundary conditions used for three methodologies are shown in Figure 3:

a) Steady-state structure



b) Steady-state thermal and structure



c) Transient state thermal and structure

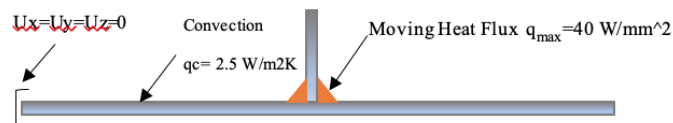


Figure III. Boundary Conditions used in three different simulation methodologies

**2.5. Geometry.** - In this study, we considered three stiffened yacht panels for simulation. The structure includes a thin plate, a girder, and a multiple stiffener arrangement. The dimensions of the plate are 1500mm x 1000mm, the girder is 1500mm x 65mm, and the stiffener is 475mm X 65mm, all with a thickness of 5 mm [25]. The dimensions of the steel plate are given in Figure 4. The CAD model of the stiffened panel was developed using SolidWorks.

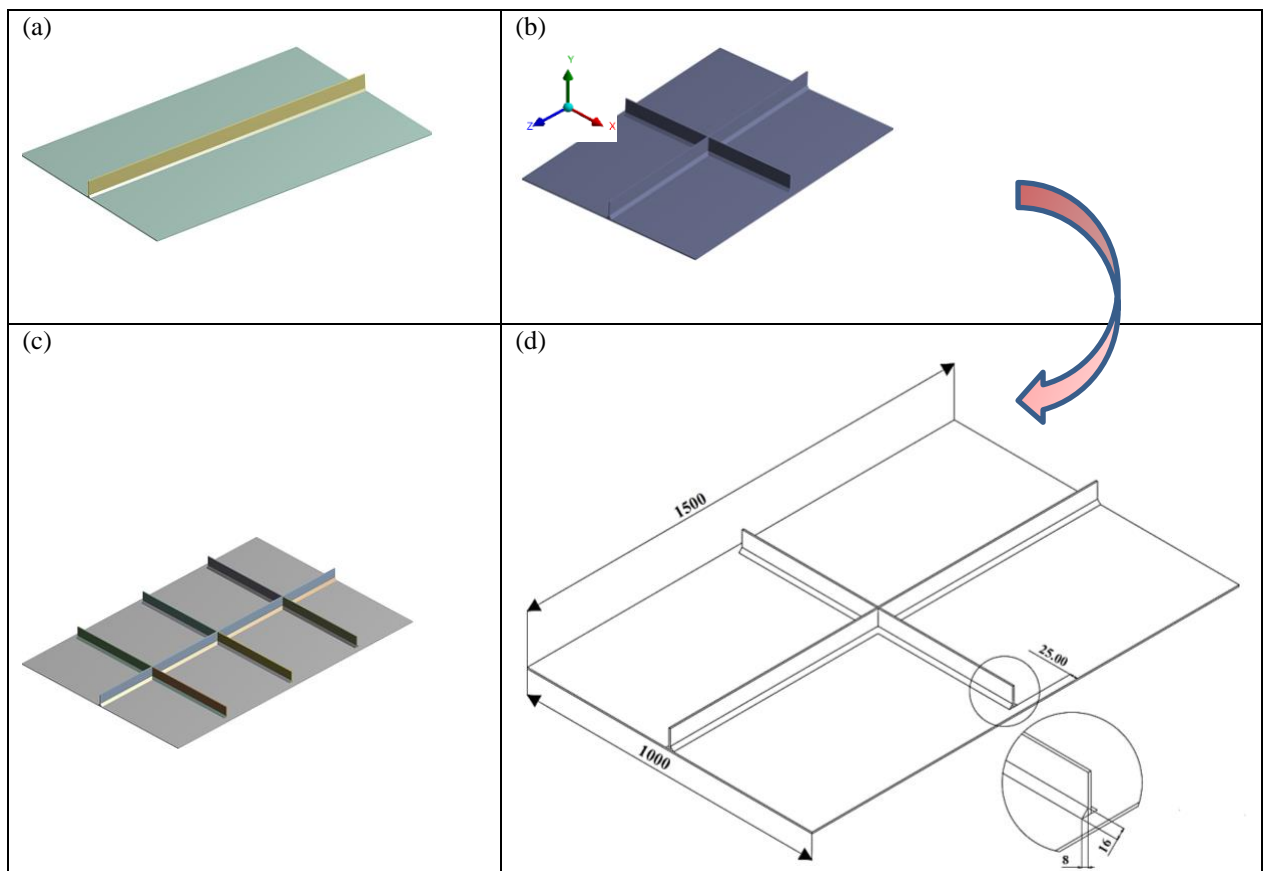


Figure IV. (a) Plate with girder, (b) plate with girder and two stiffeners, (c) plate with one girder and 6 stiffener (d) a sample 3D Cad model with detailed dimension of plate, girder and stiffener.

**2.6. Mesh.** - Overall, the mesh is comprised of non-uniform sizes and multiple thermal elements throughout the plate. Finer mesh is used close to moving heat sources, and it gradually becomes coarser closer to the end of the plates. Most refined mesh is on the welding seam region for better accuracy. To save the computational cost, appropriate mesh size was used after performing a mesh independent study. In this study, the same mesh size was used for both steady state heat transfer and transient heat transfer, i.e., the element size of weld seams and girder and thin plate was 12mm and 15 mm, respectively. A typical mesh is shown in Figure V.

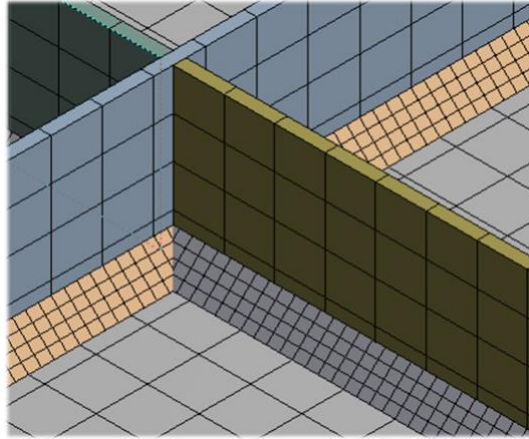


Figure V. A typical finite element mesh of of weld seams and girder and thin Plate

**2.7. Material Properties.** - The material of the panel was assumed to be Grade A36 steel. It is a common material used in shipyards and is known for its excellent mechanical properties and suitability for stiffened panels. Grade A36 offers a favorable balance of strength, ductility, and weldability, making it an ideal choice for various structural applications.

By utilizing A36 steel, we ensure the structural integrity and durability necessary for the effective performance of the ship panels in the study. Its properties are particularly beneficial in maintaining performance under the thermal and mechanical stresses associated with welding processes.

The properties of the material Grade A36 [25-27] are shown in the Table I. Gravity load is neglected in this study.

<i>Thermal Properties</i>		<i>Structural Properties</i>	
<b>Thermal Conductivity</b>	84 W/m.°C	<b>Youngs Modulus</b>	2E+11 Pa
<b>Specific Heat</b>	480 J/kg.°C	<b>Bulk Modulus</b>	1.67E+11 Pa
<b>Coefficient of Thermal Expansion</b>	1.2 e-05 C <sup>-1</sup>	<b>Poisson's Ratio</b>	0.3
		<b>Shear Modulus</b>	7.69 E+10 Pa
<i>Non-Linear Properties-Bilinear Isotropic Properties</i>			
<b>Yield Strength</b>	235 MPa		
<b>Tangent Modulus</b>	1400 MPa		

Table I. Thermo-mechanical Properties of Grade A steel

### 3. Results and Discussion. –

**3.1. Numerical Simulation.** - The numerical simulation of the welding process was carried out in this section based on the computational model developed in section 3. Thermal stresses were generated due to the heat transfer in the panel and as a result of plastic deformation. The bi-linear thermal-elastic-plastic simulation model was used in this study [28, 29]. Further extension and APDL codes were used in the latter part of the analysis to simulate transient cases [30].



The findings from this study align with other published research. For instance, a distortion simulator developed in [31] predicted welding and buckling distortion in shipbuilding with an accuracy of 80–98%. Another study [32] on aluminum hulls demonstrated that optimizing the welding sequence can reduce deformation by up to 52.1%, supporting the conclusions drawn in this research about the impact of welding sequences on minimizing distortion.

The aim of these simulations is to determine whether the proposed model can capture the welding phenomenon and how closely it can predict the welding induced deformations. Therefore, three numerical simulations methodologies were developed in this study to simulate the welding process on the yacht panels.

1. **Steady State Structure**
2. **Steady Thermal and Structure**
3. **Transient Thermal and Structure.**

Each methodology gave a different insight into the process of fabricating a thin yacht panel. Furthermore, during simulations it was explored that the following parameters affect the welding process.

- 1) Welding sequence-based deformation control
- 2) Effect of different types of Thermal Loads
  - a. Temperature
  - b. Heat Flux
  - c. Moving Heat Flux
- 3) Convection BC
- 4) Cooling phase.

In addition to the above welding process parameters, boundary conditions such as clamping location and differential heat can also affect the deformations. Following assumptions are made in simulations.

1. No phase change from solid to liquid.
2. Temperatures are maintained below the melting point of the material.

In this simulation, we assumed no phase change from solid to liquid, even though phase changes are common in welding. This assumption was made to simplify the model and reduce the complexity of the calculations.

Our main goal was to study the thermal effects and the structural behavior of the material at temperatures below its melting point, which is most relevant to this study.

By keeping the simulation within this temperature range, we could accurately model the process without adding complications related to phase changes. These assumptions are in line with the reference materials used for this research [28, 29, 30].

We also assumed that the welding process did not reach temperatures high enough to cause the material to melt. This scenario represents cases where controlled heat input is applied to avoid melting during welding. By maintaining temperatures below the material's melting point, we focused on understanding the thermal and mechanical effects without needing to model the complexities of melting and solidification. This approach is consistent with the methods used in previous research [25, 28, 29, 30].

Two boundary conditions are necessary to define the model.

1. Convection
2. Ambient Temperature of the body.

**3.2. Steady State Methodology.** - In the steady-state methodology, the temperature load was ramped from ambient 22 °C to the max. 1500 °C. This is an approximated temperature achieved by arc welding. There was uniform heating, and panels were allowed to cool and restore to initial conditions. The ends were kept fixed. The residual thermal stresses and total deformations fields were obtained during the process.

Later, I implemented a new approach that involves a **coupled analysis (steady-state Thermal + Structural Modules)** method in ANSYS. The second steady-state analysis involving both the thermal and structural modules was introduced to add additional layers of realism to the simulation.

While the initial steady-state structure methodology provided valuable insights into the structural response to temperature changes, the combined thermal-structural analysis enabled a more comprehensive understanding of how both temperature and mechanical effects interact simultaneously.

This adds "nuance" because the model now reflects how temperature changes within the material over time, influencing both thermal stresses and deformations in a more realistic way than just applying a static temperature load.

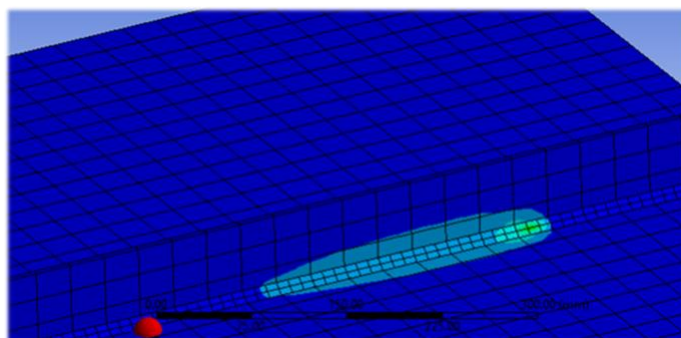
This method begins by calculating the temperature distribution through heat transfer, which is then utilized for the subsequent structural analysis.

By doing so, it enables a more realistic assessment of thermal stresses and deformations, accurately reflecting the localized heating and cooling associated with welding.

In comparison, the initial method presents a simplified perspective, assuming a uniform heat distribution, whereas the new approach integrates dynamic heat transfer, yielding more detailed insights into the thermal and mechanical behavior during the welding process.

**3.3. Transient Methodology.** - The purpose of this study was to develop a numerical model that captured the physics of welding process on a ship panel, i.e., the distortions and stresses must be simulated closer to the real process. Here the transient load was considered. A thermal load was not only a function of time but also a function of position as well.

A moving heat arc in welding travels through to the joint with speed defined by a welding machine or in a more conventional sense, by a welder. This moving heat source can only be simulated in Transient Modules of ANSYS. Figure 6 shows the moving heat flux in ANSYS. The velocity was defined by the speed at which the moving heat flux travels the weld bead. In practical life, it was adjusted by the welding machine, or estimation can be made considering the speed at which welders weld.



*Figure VI. A typical shape of moving heat flux*

Source power intensity was defined by the type of weld. It can also be adjusted to achieve the relevant temperatures of particular welding. Start time and end time were crucial, so it was defined by the classical equation of motion, i.e., distance=velocity x time.

The sequence of welds plays an important role. This can reduce the deformation in the structure [25]. Unlike the steady-state process, the transient analysis runs for the entire duration of the process. The welding sequence used in the current study is shown in Figure 7.

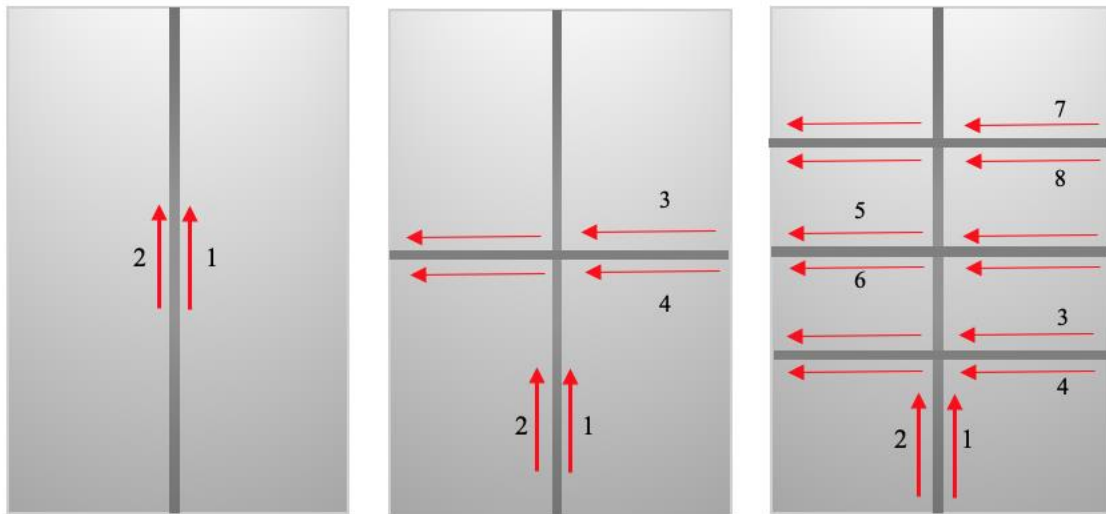


Figure VII. Welding Sequence followed in the numerical simulations.

Table II shows the comparison between the capability of different methodologies in capturing the total deformation in the panel. Result legends are different for steady-state and transient methods. Two trends can be seen, from left, to right the deformation is controlled. From Top to Bottom Effectiveness of methodologies in capturing the results and better deformation distribution can be seen.

Table II (a) case 01 (steady-state structure) presents the deformation caused by the heat load. This means rectification will be needed in real life for the panel to be used in ship construction. As expected, most deformation occurs at the loaded area. The maximum deformation occurred at peak load. In this methodology, the plastic deformation is reduced after the unloading of thermal loads as seen in Figure VIII. Table II (b) case 02 (steady-state structure) has additional stiffeners in the mid-section of the panel. This generated more stress and resulted in larger deformation. The girder and stiffener areas were largely affected regions. Areas that were fixed have little to no deformation. This shows the clamping has a positive effect on the control of deformation. Figure VIII shows a similar trend of deformation for case 02 as in the previous case. In Table II (c) case 03 (steady-state structure), the deformation was concentrated at the center of the panel, but the overall effect was lower than both case 01 (a) and case 02 (b). Figure VIII showed a trend that the deformation was reducing as more stiffeners were added, this happened due to the extra rigidity added by the stiffeners.

Table II (d), (e), and (f) case 01, case 02, and case 03 respectively also represents a steady-state methodology but with coupled thermal and structure modules in ANSYS. This helps in the introduction of heat flux as load and more detailed boundary conditions. The deformation becomes larger which means adding details to the methodologies reveals more information.

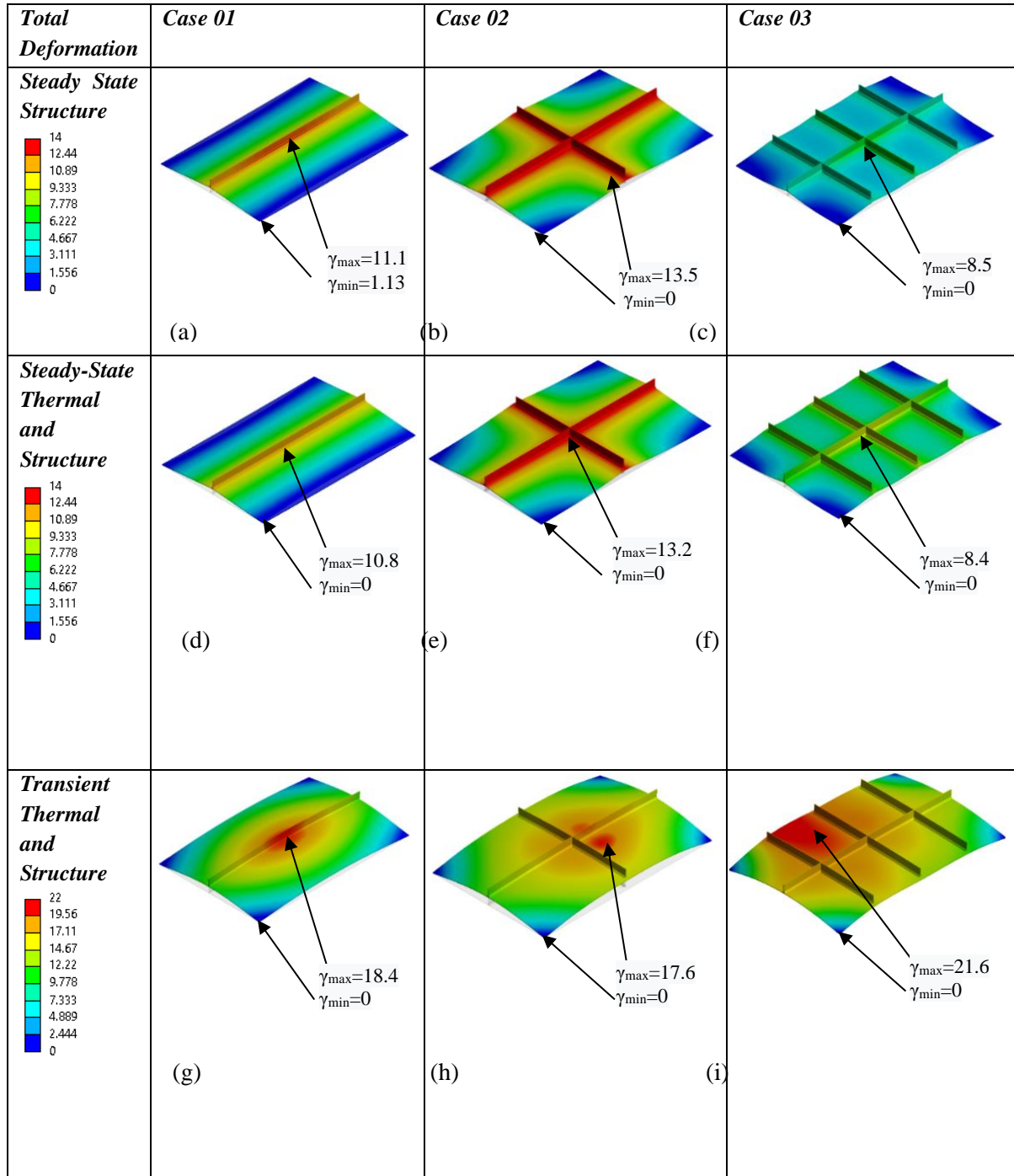


Table II. Total Deformation in panels.

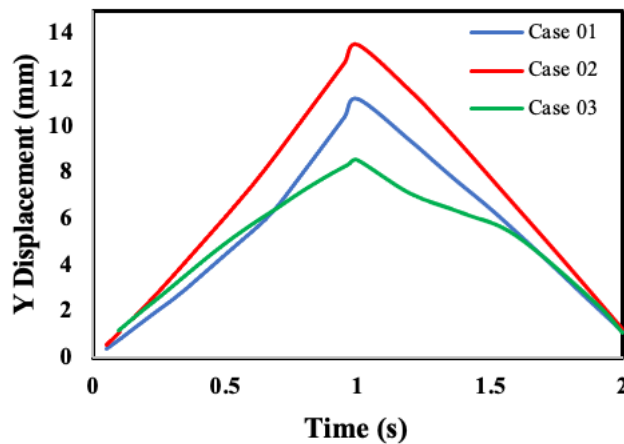


Figure VIII. Deformation Steady State at the maximum displacement location.

Transient Analysis gives the most accurate and detailed analysis of the physical phenomenon occurring in the results. The contours are more detailed and closer to reality. The flexibility to introduce other factors like convection, clamping, cooling, differential heat, and moving heat sources, made it a suitable choice.

In Table III (g) case 01 the transient analysis captures the deformation of the panel more accurately. In previous cases, the deformation occurred on girder and stiffeners but here a collective deformation of the panel can be seen. Mainly the deformation concentration was at the center of the plate. The panel was permanently de-shaped which is an actual occurrence in the fabrication of ship panels. The cooling effect did not reduce the deformation radically as in the steady-state case. It reached a peak of ~19 mm and cooling reduced it to ~17mm as seen in Figure IX. It can also be seen in Figure IX that the initial and endpoints are different. The unloading of loads in the transient case did not reduce the deformation and plastic deformation was captured.

Table III (h) case 02 followed the same trend and showed an increase in deformation. The deformation concentration in this analysis was seen to be distributed more realistically and did not reduce at all in the cooling phase. The previous cases showed a trend of increased deformation with the addition of extra stiffeners. In Table III (i) case 03 controlling the parameters like sequence, clamping, the convection effect can reduce the overall deformation as seen in the results. **The results were in agreement with the experimental results and show only a 5% of deviation [25].**

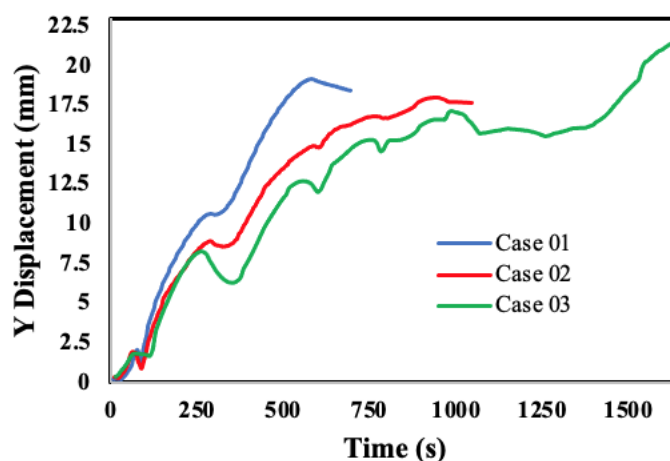


Figure IX. Deformation Transient State.

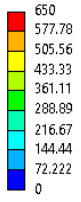
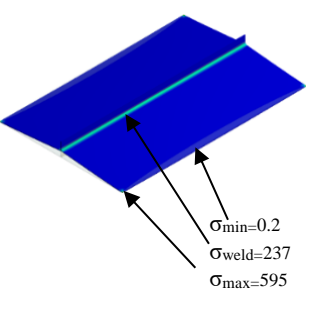
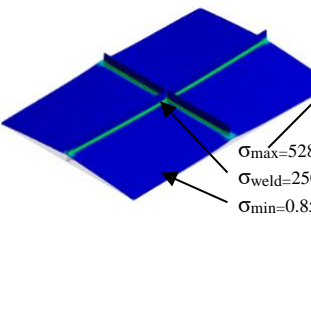
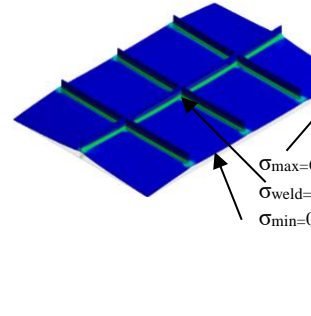

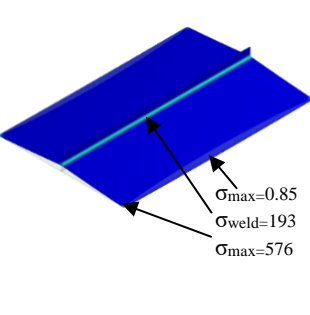
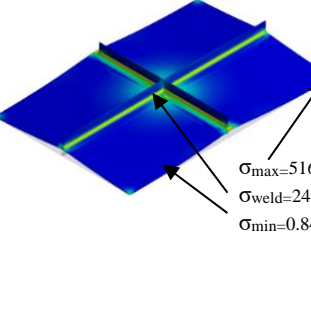
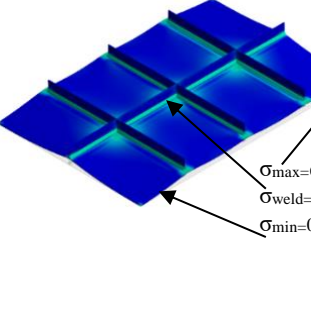
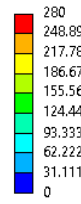
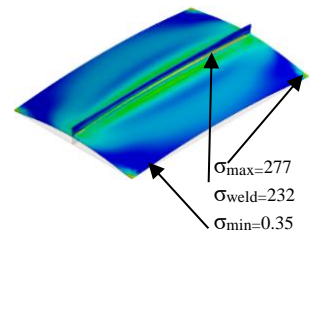
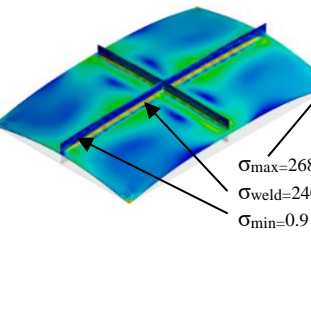
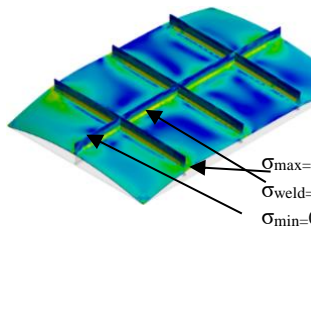
Thermal Stresses	Case 01	Case 02	Case 03
<b>Steady State Structure</b> 	 <p><math>\sigma_{min}=0.2</math> <math>\sigma_{weld}=237</math> <math>\sigma_{max}=595</math></p> <p>(a)</p>	 <p><math>\sigma_{max}=528</math> <math>\sigma_{weld}=250</math> <math>\sigma_{min}=0.85</math></p> <p>(b)</p>	 <p><math>\sigma_{max}=630</math> <math>\sigma_{weld}=241</math> <math>\sigma_{min}=0.17</math></p> <p>(c)</p>
<b>Steady-State Thermal and Structure</b> 	 <p><math>\sigma_{max}=0.85</math> <math>\sigma_{weld}=193</math> <math>\sigma_{max}=576</math></p> <p>(d)</p>	 <p><math>\sigma_{max}=516</math> <math>\sigma_{weld}=248</math> <math>\sigma_{min}=0.84</math></p> <p>(e)</p>	 <p><math>\sigma_{max}=635</math> <math>\sigma_{weld}=245</math> <math>\sigma_{min}=0.85</math></p> <p>(f)</p>
<b>Transient Thermal and Structure</b> 	 <p><math>\sigma_{max}=277</math> <math>\sigma_{weld}=232</math> <math>\sigma_{min}=0.35</math></p> <p>(g)</p>	 <p><math>\sigma_{max}=268</math> <math>\sigma_{weld}=240</math> <math>\sigma_{min}=0.9</math></p> <p>(h)</p>	 <p><math>\sigma_{max}=236</math> <math>\sigma_{weld}=200</math> <math>\sigma_{min}=0.69</math></p> <p>(i)</p>

Table III. Thermal Stresses

In Table III (a) case 01, it can be seen that the majority of the stresses were along with the weld bead, there was a minute effect of welding at the fixed corners. Figure X gives a qualitative view of the thermal stresses which reach out to 500 MPa and was well above the plastic limit. It is to be noted that the stresses reduce as the cooling phase starts, the reduction of stresses does not go to the level of the initial state, and there remain the residual stresses in the panel. In Table III (b) case 02 a larger stress concentration was observed at the corners and the middle of the panel while the weld seams remain dominant in stress as expected also residual stresses are larger in this case. In Table III (c) case 03

The thermal stresses were mainly concentrated at the weld part; the distribution was larger as compared to previous cases. The stresses reach the peak value of  $>600$  MPa as seen in Figure X but the cooling phase reduces the majority of the stresses. There was a considerable amount of residual stress.

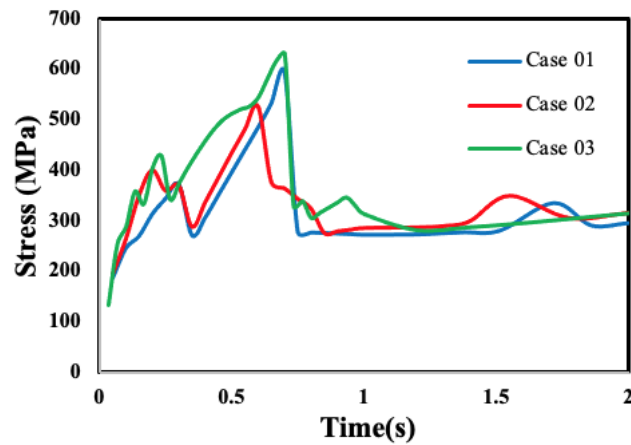


Figure X. Thermal Stresses Steady State.

Table 3 (d) case 01, 3 (e) case 02, and 3 (f) case 03 reveals a higher value of stresses. This was due to the introduction of heat flux, and convection which better captures the physical phenomenon.

In Table III (g) case 01 the stresses captured represented the right trends. The previous methodologies captured the stress concentration at the corners (fixed ends). But the values were extremely large and hence suggested an error. The transient case also showed a similar trend, but the values were just above the yield strength of the material which was reasonable. This suggested that excessive plastic deformation is present at the corners. The values in Table III (a to f) are high enough to cause a fracture. As seen in Figure XI there is a fluctuation in stresses throughout the simulation. It was because of the following reasons: The nonlinearity of the system and transient nature of simulation. This causes instability to the system which affects the results. This can be reduced by adopting the following measure, i.e., refined Mesh and decreased the step size. Although these measures will significantly increase the computational time of the process. The graph in Figure XI also represents the cooling time taken by the different methodologies. The diamond shape legend shows the start of cooling of a panel due to natural convection.

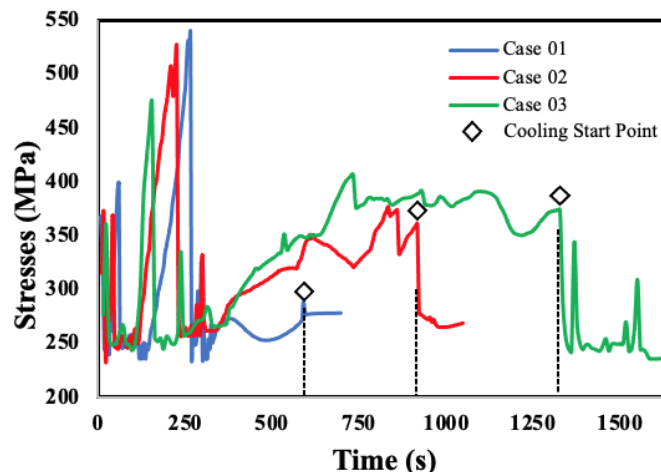


Figure XI. Thermal Stresses Transient State.

Table III (h) shows thermal stresses that agree with the ongoing trend. The max value of stress is less. The overall stress values were lower than those captured in previous methodologies.

This also showed that the right sequence of welds can reduce the residual stress considerably. Table 3 (i) was the most complex case of all and required much more computational time.

The stress concentration at the corners was very high. The sequential weldment of stiffeners can reduce overall residual stresses and deformation. The residual stresses were present and at some points were above the yield strength of the material. But the majority of the area was less affected.

**4. Conclusion.** - In this study we concluded that the thermo-mechanical modeling approach with transient heat transfer analysis with moving source and elastic-plastic material model are an optimal solution to carry out prediction study of deformation and residual stresses. The deformation acquired with the proposed models were compared with results of deformation from the literature. Good agreement in the deformation results were observed with error of less than 5% [17]. This validates the numerical model of the analysis.

The study highlights several key findings. First, temperature loads in the steady-state heat transfer analysis may not fully represent real manufacturing conditions due to uniformity not being observed in practice. However, using a moving heat flux overcomes this limitation by better simulating real welding scenarios. Second, the sequentially coupled transient thermal and structure module in ANSYS offers a more accurate depiction of the welding process, with numerical results closely matching experimental data (within 5% accuracy) [17]. Lastly, the control of parameters like weld sequence, cooling, and clamping significantly influences deformation. Panels with more stiffeners, despite their complexity, performed better in this study. These findings underscore the importance of optimizing these factors to enhance welding outcomes. Future research could explore refining these simulations for other materials or welding techniques, further improving accuracy and industrial applicability.



## References

- [1] K. Fattaneh Morshedsolouk, Mohammad, "Parametric study on average stress-average strain curve of composite stiffened plates using progressive failure method," *Latin American Journal of Solids and Structures*, 2014.
- [2] B. C. Cerik, S.-R. J. J. o. m. S. Cho, and Technology, "Numerical investigation on the ultimate strength of stiffened cylindrical shells considering residual stresses and shakedown," vol. 18, no. 4, pp. 524-534, 2013.
- [3] S. Li and S. J. O. E. Benson, "The influence of residual stress on the ultimate strength of longitudinally compressed stiffened panels," vol. 231, p. 108839, 2021.
- [4] D. Podder, O. P. Gupta, S. Das, and N. R. J. W. i. t. W. Mandal, "Experimental and numerical investigation of effect of welding sequence on distortion of stiffened panels," vol. 63, no. 5, pp. 1275-1289, 2019.
- [5] M. M. Khalilabad, Y. Zedan, D. Texier, M. Jahazi, and P. J. J. o. M. P. Bocher, "Effect of tool geometry and welding speed on mechanical properties of dissimilar AA2198-AA2024 FSWed joint," vol. 34, pp. 86-95, 2018.
- [6] T. Tchoumi, F. Peyraut, and R. J. J. o. M. P. T. Bolot, "Influence of the welding speed on the distortion of thin stainless steel plates—Numerical and experimental investigations in the framework of the food industry machines," vol. 229, pp. 216-229, 2016.
- [7] V. Farajkhah and Y. J. T. I. J. o. A. M. T. Liu, "Effect of clamping area and welding speed on the friction stir welding-induced residual stresses," vol. 90, no. 1, pp. 339-348, 2017.
- [8] U. Kumar, D. Gope, J. Srivastava, S. Chattopadhyaya, A. Das, and G. J. M. Krolczyk, "Experimental and numerical assessment of temperature field and analysis of microstructure and mechanical properties of low power laser annealed welded joints," vol. 11, no. 9, p. 1514, 2018.
- [9] Z. Chen, Z. Chen, and R. A. J. O. E. Sheno, "Influence of welding sequence on welding deformation and residual stress of a stiffened plate structure," vol. 106, pp. 271-280, 2015.
- [10] Y. Zhang and Y. J. M. S. Wang, "The influence of welding mechanical boundary condition on the residual stress and distortion of a stiffened-panel," vol. 65, pp. 259-270, 2019.
- [11] Y. Kim, J. Kim, and S. J. A. S. Kang, "A study on welding deformation prediction for ship blocks using the equivalent strain method based on inherent strain," vol. 9, no. 22, p. 4906, 2019.
- [12] K. Masubuchi and N. J. W. J.-.-N. Y.-.-. Ich, "Computer analysis of degree of constraint of practical butt joints," vol. 49, no. 4, p. 166, 1970.
- [13] C. Wu and J.-W. J. T.-W. S. Kim, "Numerical prediction of deformation in thin-plate welded joints using equivalent thermal strain method," vol. 157, p. 107033, 2020.
- [14] L. Li, D. Liu, S. Ren, H.-g. Zhou, and J. J. S. Zhou, "Prediction of Welding Deformation and Residual Stress of a Thin Plate by Improved Support Vector Regression," vol. 2021, 2021.
- [15] S. J. S. Zhang and O. Structures, "A review and study on ultimate strength of steel plates and stiffened panels in axial compression," vol. 11, no. 1, pp. 81-91, 2016.
- [16] W.-y. Wang, B. Liu, and V. J. J. o. m. i. c. e. Kodur, "Effect of temperature on strength and elastic modulus of high-strength steel," vol. 25, no. 2, pp. 174-182, 2013.
- [17] M. T. Ali and R.-F. J. A. o. D. d. J. U. o. G. F. X. S. Teodor, "Control of welding deformation in thin plate," vol. 41, pp. 113-120, 2018.
- [18] K. Niklas and J. J. O. e. Kozak, "Experimental investigation of Steel–Concrete–Polymer composite barrier for the ship internal tank construction," vol. 111, pp. 449-460, 2016.
- [19] Y. Liu, N. Ma, F. Lu, and H. J. J. o. M. P. Fang, "Measurement and analysis of welding deformation in arc welded lap joints of thin steel sheets with different material properties," vol. 61, pp. 507-517, 2021.
- [20] J. D. Russell, "Application of laser welding in shipyards," in *Lasers in Material Processing*, 1997, vol. 3097, pp. 174-183; International Society for Optics and Photonics.
- [21] N. J. J. o. s. p. McPherson, "Thin plate distortion—the ongoing problem in shipbuilding," vol. 23, no. 02, pp. 94-117, 2007.
- [22] Z. Samad, N. Nor, and E. Fauzi, "Thermo-Mechanical Simulation of Temperature Distribution and Prediction of Heat-Affected Zone Size in MIG Welding Process on Aluminium Alloy EN AW 6082-T6," in *IOP Conference Series: Materials Science and Engineering*, 2019, vol. 530, no. 1, p. 012016; IOP Publishing.
- [23] D. Kollár, B. G. Kövesdi, and J. J. P. P.-C. E. Nézö, "Numerical simulation of welding process—application in buckling analysis," vol. 61, no. 1, pp. 98-109, 2017.

- [24] A. Support. (2021). *Moving Heat Source*. Available: <https://catalog.ansys.com/product/5b3bc6857a2f9a5c90d32e7e/moving-heat-source?creator=ANSYS%20Inc>
- [25] A. M. Taha, "Experimental Analysis To Control Welding Deformation In Thin Plate," in *International Conference on Computer Applications in Shipbuilding*, 2019, vol. 2019, pp. 24-26.
- [26] T. Sirisatien, S. Mahabunphachai, and K. J. M. T. P. Sojiphan, "Effect of submerged arc welding process with one-side one-pass welding technique on distortion behavior of shipbuilding steel plate ASTM A131 grade A," vol. 5, no. 3, pp. 9543-9551, 2018.
- [27] A. Mostafanejad, M. Iranmanesh, and A. J. O. E. Zarebidaki, "An experimental study on stress corrosion behavior of A131/A and A131/AH32 low carbon steels in simulated seawater," vol. 188, p. 106204, 2019.
- [28] H. Nishikawa, I. Oda, M. Shibahara, H. Serizawa, and H. Murakawa, "Three-dimensional thermal-elastic-plastic FEM analysis for predicting residual stress and deformation under multi-pass welding," in *The Fourteenth International Offshore and Polar Engineering Conference*, 2004: OnePetro.
- [29] S. S. Antman, "Nonlinear plasticity," in *Nonlinear Problems of Elasticity*: Springer, 1995, pp. 603-628.
- [30] A. Savas. (2021). *Ansys apdl code for moving heat source*. Available: [https://www.researchgate.net/post/Ansys\\_apdl\\_code\\_for\\_moving\\_heat\\_source\\_in\\_welding\\_simulation\\_having\\_problem\\_for\\_local\\_coordinate\\_system](https://www.researchgate.net/post/Ansys_apdl_code_for_moving_heat_source_in_welding_simulation_having_problem_for_local_coordinate_system)
- [31] Lee, C., S. Woo, and J. Kim, Impact Analysis of Welding Sequence to Reduce Weld Deformation in Aluminum Hulls. *Journal of Marine Science and Engineering*, 2024. 12(9): p. 1604.
- [32] Cheon, Y.-J., B.-G. Kang, and D.-J. Lee. An Automatic Welding and Buckling Distortion Analysis Using 3D-CAD Models of Hull Structure. in *ISOPE International Ocean and Polar Engineering Conference*. 2023. ISOPE.

**Author contribution:**

1. Conception and design of the study
2. Data acquisition
3. Data analysis
4. Discussion of the results
5. Writing of the manuscript
6. Approval of the last version of the manuscript

SA has contributed to: 1, 2, 3, 4, 5 and 6.

MA has contributed to: 1, 2, 3, 4, 5 and 6.

AAZ has contributed to: 1, 2, 3, 4, 5 and 6.

**Acceptance Note:** This article was approved by the journal editors Dr. Rafael Sotelo and Mag. Ing. Fernando A. Hernández Goberti.